iScience

Article

UFMylation maintains YAP stability to promote vascular endothelial cell senescence

Graphical abstract

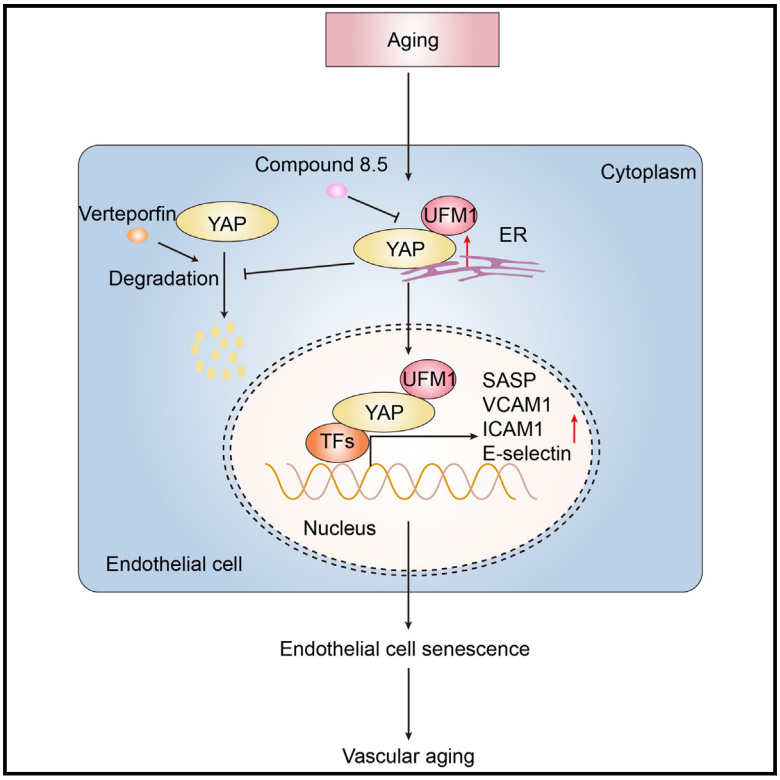

Highlights

- YAP and UFM1 are elevated in senescent endothelial cells
- YAP was identified as a substrate of UFMylation, which maintains its stability
- UFM1-modified YAP was elevated in senescent ECs
- Inhibiting YAP-UFMylation improves the cardiovascular aging phenotype in aged mice

Authors

Yanan Liu, Min Zuo, Aiwei Wu, ..., Yongping Bai, Junzhi Zhou, Hu Wang

Correspondence

baiyongping@csu.edu.cn (Y.B.), zhoujunzhi2013@163.com (J.Z.), wanghu19860315@163.com (H.W.)

In brief

Biological sciences; Biochemistry; Cell biology; Cell

Liu et al., 2025, iScience *28*, 111854
February 21, 2025
https://doi.org/10.1016/j.isci.2025.111854

CellPress

iScience

CellPress
OPEN ACCESS

Article

UFMylation maintains YAP stability to promote vascular endothelial cell senescence

Yanan Liu,[1,2] Min Zuo,[2] Aiwei Wu,[2] Zhaoxiang Wang,[3] Siting Wang,[1] Yongping Bai,[1,*] Junzhi Zhou,[3,*] and Hu Wang[2,4,*]
[1]Department of Geriatric Medicine, Center of Coronary Circulation, Xiangya Hospital, Central South University, Changsha, Hunan 410008, China
[2]Key Laboratory of Aging and Cancer Biology of Zhejiang Province, Institute of Aging Research, School of Basic Medicine Sciences, Hangzhou Normal University, Hangzhou 311121, China
[3]School of Basic Medicine, Guangdong Medical University, Dongguan 523808, China
[4]Lead contact
*Correspondence: baiyongping@csu.edu.cn (Y.B.), zhoujunzhi2013@163.com (J.Z.), wanghu19860315@163.com (H.W.)
https://doi.org/10.1016/j.isci.2025.111854

SUMMARY

Endothelial cell (EC) senescence is an accomplice for vascular aging, which leads to cardiovascular diseases (CVDs). Evidences showed that Hippo-Yes-associated protein (YAP) signaling pathway plays an essential role in aging-associated CVDs. Here, we reported that YAP was elevated in senescent human umbilical vein endothelial cells (HUVECs) and inhibition of YAP could attenuate HUVECs senescence. Besides, our findings revealed that the activity of UFMylation and the level of YAP were both elevated in senescent cells. Furthermore, UFM1-modified YAP was upregulated in senescent ECs, and increased the stability of YAP. Importantly, we found that compound 8.5, an inhibitor of E1 of UFMylation, can alleviate vascular aging in aged mice. Together, our finding provides molecular mechanism by which UFMylation maintains YAP stability and exerts an important role in promoting cell senescence, and identified that a previously unrecognized UFMylation is a potential therapeutic target for anti-aging.

INTRODUCTION

Cardiovascular disease (CVD) is the leading cause of death worldwide, with an estimated 17.9 million people dead from CVD in 2019, accounting for 32% of all deaths worldwide, and vascular dysfunction is a key feature.[1] The vascular is made up of tunica intima, tunica media, and tunica adventitia. The tunica intima consists mainly of a single layer of endothelial cells (ECs) and a basement membrane.[2] ECs not only act as a barrier between circulation and peripheral tissues, but also play important physiological roles in vascular homeostasis, maintenance of blood flow, regulation of vascular tone, pro-inflammatory response, and neovascularization.[3] Dysfunction of ECs is the cause of human angiocardiopathy and has been identified as an important contributor to CVD.

It has been demonstrated that EC senescence is associated with aging process that leads dysfunction of ECs when aging occurs.[4] Senescent ECs generally exhibit typical hallmarks of senescent cells, such as flattened and enlarged morphology, increased polyploidy, produce a complex senescence-associated secretory phenotype (SASP), increased SA-β-gal activation and expression of p16/p21.[5] Besides, senescent ECs secret large amounts of soluble adhesion molecules and inflammatory molecules, which promote the adherence of inflammatory cells to the vasculature, thereby inducing vascular inflammation and contribute to arterial dysfunction and aging, thus increased risk of aging-related CVD such as atherosclerosis and hypertension.[6–10] So far, the mechanism by which EC senescence has being regulated during aging remains fully unclear.

The Hippo pathway, discovered in *Drosophila*, controls the size of organs by regulating the survival, proliferation, and apoptosis of cells.[11] The *Drosophila* Hippo pathway is highly conserved in mammals, and Yes-associated protein (YAP) is a key functional effector of the Hippo pathway in the mammalian.[12] Either smooth muscle cells (SMCs)- or ECs-specific knockout of YAP resulted in impaired cardiovascular system development in mice, suggesting that YAP has an important role in the development and homeostasis of the cardiovascular system.[13–15] Moreover, YAP was also found to contribute to aging-related cardiovascular disease such as atherosclerosis, hypertension, and arterial stiffness. YAP promote ECs secretion of large amounts of soluble adhesion molecules (ICAM-1, VCAM-1, and E-selectin), initiating an inflammatory process in the vessel wall toward atherosclerosis.[16,17] The suppression of mTORC1 activity in ECs increased autophagic degradation of YAP and thus reduced YAP-mediated COX-2/mPGES-1 expression that resulted in hypertension.[18] YAP facilitates pressure overload-induced dysfunction in the diabetic heart.[19] Our previous study showed that a high-fat, high-sugar diet reduces autophagy-mediated degradation of YAP in SMCs and promotes sustained activation of the transforming growth factor β (TGF-β)/Smad signaling pathway to induce arterial stiffness in mice.[20] Disruption of the YAP/TEAD complex promotes the senolysis of senescent cells in aging mice, and increased YAP activity promotes

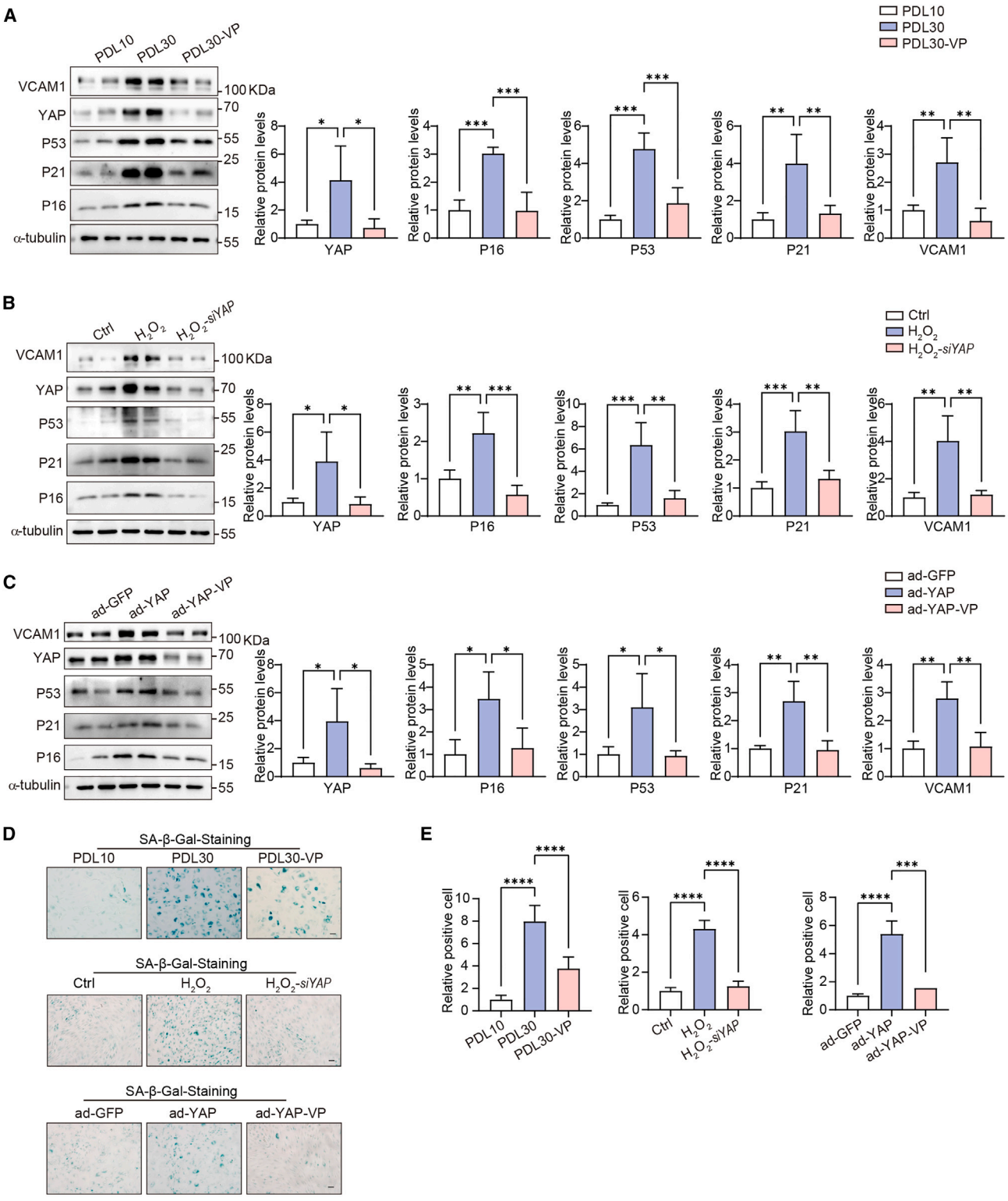

Figure 1. YAP was upregulated in senescent endothelial cells

(A) The proliferation of HUVECs population doubling level (PDL) at 10 and 30 were treated with vehicle or verteporfin (0.5 μM) for 12 h. Immunoblotting and quantifying the protein level of P16, P21, P53, VCAM1, and YAP. $n = 4$.

(legend continued on next page)

chronic inflammation-induced ECs senescence.[21,22] However, the role of YAP in the natural aging of ECs and vascular is not fully understood.

The UFMylation pathway is a less-studied ubiquitin-like molecules (UBLs), toward regulate the stability and function of proteins, which is essential for maintaining cell development and tissue homeostasis.[23,24] The core molecules involved in the UFMylation pathway, including ubiquitin-fold modifier 1(UFM1), UFM1-specific cysteine proteases (UFSP2), E1 ubiquitin-activating enzyme 5 (UBA5), E2 UFM1-conjugase 1 (UFC1), and E3 UFM1-ligase 1 (UFL1).[25] UFMylation increases the stability of the tumor suppressor p53 to exert a tumor suppressor function.[26] UFMylation as an important mediator of the endoplasmic reticulum (ER) stress response, both the protective effect in heart failure and the inhibition of interferon-gamma (IFN-γ)-induced macrophage activation are mediated by inhibition of ER stress.[27,28] Moreover, the latest research shows that the UFMylation system has important functions in the recruitment of GPCRs to COPII vesicles, in biosynthetic transport and in sorting at the ER via the UFMylation and direct interaction of UFBP1.[29] We recently reported that dysregulation of PD-L1 by UFMylation imparts tumor immune evasion and identified as a potential therapeutic target.[30] So far, only a few UFMylation substrates have been described. The substrates of UFMylation and their potential biological relevance, particularly in ECs senescence, remain poorly understood.

In this study, we found that YAP is elevated in both senescence cells of human umbilical vein endothelial cells (HUVECs) and aging vascular of mice. Importantly, we found that UFMylation maintain YAP stability increased its protein stability and thus promoted ECs senescence, whereas administration of compound 8.5, an inhibitor of UFMylation, and an inhibitor of YAP retarded ECs senescence. In addition, *in vivo*, compound 8.5 attenuated vascular aging and improved heart function in aged mice. These findings indicate that targeting the UFMylation of YAP might be an effective strategy to prevent ECs senescence along with vascular aging.

RESULTS

YAP upregulated in senescent vascular endothelial cell and inhibition of YAP attenuated cell senescence

YAP signaling pathway has been shown to play an important role in a variety of CVDs including the aging-related CVDs atherosclerosis and hypertension.[17,31–35] However, the exact role of YAP in vascular ECs senescence remains to be answered. To investigate the role of YAP in vascular ECs senescence, we used serial passaging to create a model of HUVECs senescence, young cells (PDL10) and senescent cells (PDL30) were analyzed.[36] Our immune-blot showed that significantly upregulated expression of YAP with elevated P16, P21, P53 and VCAM1 in senescent HUVECs. Furthermore, verteporfin (VP), an inhibitor of YAP, which attenuated the expression of YAP with reduced P16, P21, P53, and VCAM-1 (Figure 1A). To further mimic the senescence of ECs, we treated HUVECs with H_2O_2 and also found that YAP was upregulated expression in H_2O_2-induced senescent cells with elevated P16, P21, P53, and VCAM-1 (Figure 1B). Similarly, knockdown of endogenous YAP by specific small interfering RNA (siRNA) attenuated the expression of YAP with reduced P16, P21, P53, and VCAM-1 (Figure 1B). Last but not least, adenovirus-mediated overexpression of YAP protein induces HUVECs senescence with elevated P16, P21, P53, and VCAM-1 compared with controls (Figure 1C). Importantly, senescence-associated β-galactosidase (SA-β-Gal) staining in HUVECs also suggested that inhibition of YAP protein attenuated ECs senescence (Figures 1D and 1E). Together, our aforementioned results found that YAP was upregulated in several models of senescence ECs and inhibition of YAP could attenuates ECs senescence and suggested that ECs-YAP may be a potential therapeutic target for anti-vascular aging.

YAP was identified as a substrate for UFMylation

It has been reported that YAP subjected several PTM modifications (e.g., ubiquitination, phosphorylation, O-GlcNAcylation, and SUMOylation),[37] suggesting PTM plays an important role in regulating YAP function. To unbiased identify the regulator of YAP, we first screen the BioGrid (https://thebiogrid.org), a biomedical interaction repository with data compiled through comprehensive curation efforts, and found that YAP could binding at UFM1 with relative high score (Figure S1A). Moreover, visualization and integrated discovery (DAVID) was used to analyze the functional annotation of YAP binding proteins and we found that protein translational modifications (PTMs) (including UFMylation genes), molecular function, cellular component, and biological process were significantly enriched. These data suggest that YAP may interact with UFM1 and subjected with modification of UFMylation (Figure S1B). Therefore, we speculate that UFM1 could cooperate with YAP in ECs. In line with our hypothesis, we observed that YAP and UFMylation activity were both upregulated in senescent cells with elevated P16, P21, P53, and VCAM-1 compared with young HUVECs (Figures 2A and 2B). In addition, the expression of downstream target genes of YAP was increased in senescent HUVECs (Figure S1C). To further explore the relationship between the YAP and UFMylation *in vivo*, we isolated aortic ECs from young and aged mice to determine the levels of the aforementioned proteins; we observed similar findings to those described previously in HUVECs (Figures 2A and 2B). A growing number of evidences showed that UFMylation, similar to ubiquitin and ubiquitin-like

(B) Proliferation of HUVECs PDL at 10 were transfected with siRNA-NC (negative control) or siRNA against YAP for 12 h, followed by treated with vehicle or H_2O_2 (100 μM) for 12 h. Immunoblotting and quantifying the protein level of P16, P21, P53, VCAM1, and YAP. $n = 4$.

(C) Proliferation of HUVECs PDL at 10 were infected with GFP adenovirus (Ad-GFP) or YAP adenovirus (Ad-YAP) for 24 h and then treated with vehicle or verteporfin (0.5 μM) for 12 h. Immunoblotting and quantifying the protein level of P16, P21, P53, VCAM1, and YAP. $n = 4$.

(D and E) SA-β-Gal staining and quantitative analysis of senescent cells, scale bars: 40 μm, $n = 6$, p values correspond to one-way ANOVA with Tukey's multiple comparisons test.

All data are represented as mean ± SEM. *, $p \leq 0.05$; **, $p \leq 0.01$; ***, $p \leq 0.001$; ****, $p \leq 0.0001$.

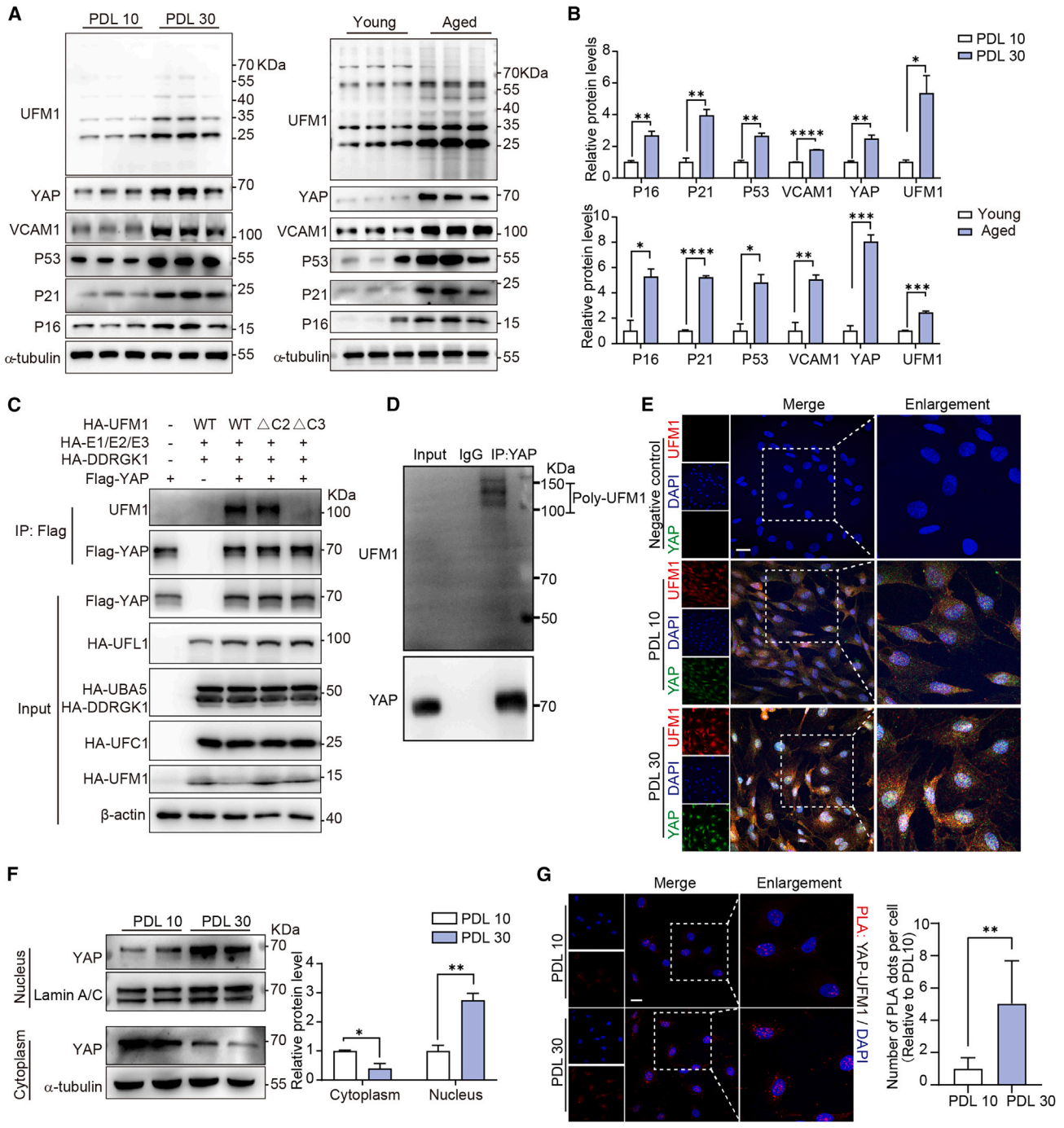

Figure 2. YAP was identified as the substrate for UFMylation

(A and B) Immunoblotting and quantification of the level of the indicated protein in HUVECs of the proliferation of PDL at 10 and 30; immunoblotting and quantification of levels of the indicated protein in aortic endothelial cells from 2 (young) or 24 (aged) months old mice. $n = 3$.

(C) HEK293T cells were co-transfected with UFMylation components (UBA5, UFC1, UFL1, and DDRGK1) or wild-type (UFM1WT) or active UFM1 (UFM1ΔC2) or defective UFM1 (UFM1ΔC3) and FLAG-tagged YAP for detection exogenous YAP UFMylation.

(D) Isolation of aortic endothelial cells from 8-week-old C57BL/6J mice for detection endogenous YAP UFMylation.

(E) Immunofluorescence staining of YAP (green), UFM1 (red), and DAPI (blue) in HUVECs of the proliferation of PDL at 10 and 30, and serum stimulation as control, scale bars: 20 μm.

(F) Isolated the nucleus and cytoplasmic proteins from young and senescent HUVECs, immunoblotting and quantification of levels YAP. $n = 4$.

(G) UFMylation detection of YAP was identified using a PLA with UFM1 and YAP antibodies. $n = 6$, p values correspond to unpaired two-tailed Student's t test. All data are represented as mean ± SEM. *, $p \leq 0.05$; **, $p \leq 0.01$; ***, $p \leq 0.001$; ****, $p \leq 0.0001$.

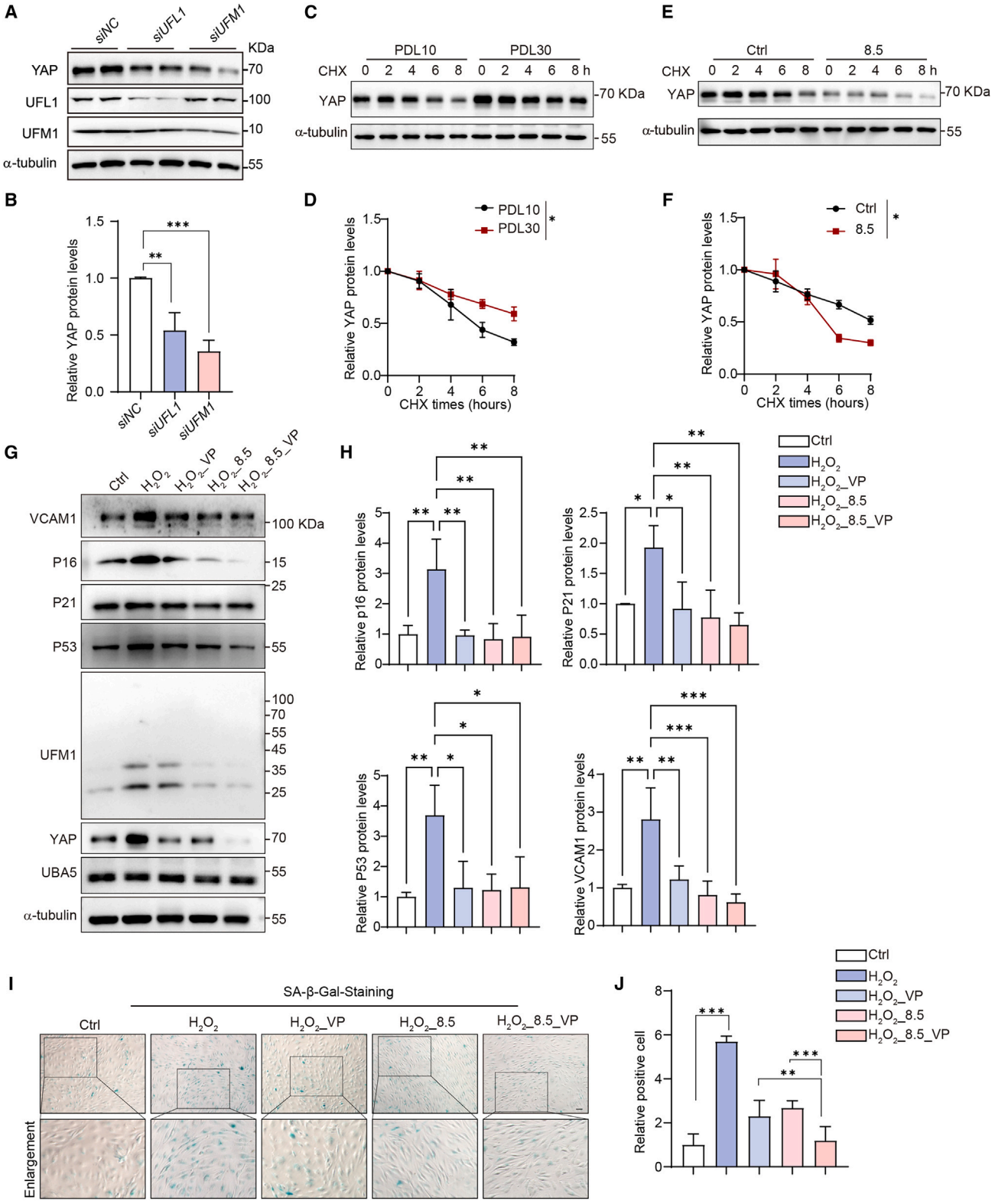

Figure 3. UFMylation of YAP slows down its protein degeneration speed and inhibiting UFMylation could prevent endothelial cell senescence

(A and B) Proliferation of HUVECs PDL at 10 were transfected with siRNA-NC (negative control) or siRNA against UFL1/UFM1 for 36 h. Immunoblotting and quantifying the protein level of YAP, $n = 4$, p values correspond to one-way ANOVA with Tukey's multiple comparisons test.

(legend continued on next page)

protein modifications, contributes to functional regulation of substrates and thus regulates a range of biological processes. Therefore, we are curious whether YAP is a substrate of UFMylation. We transiently co-expressed FLAG-tagged YAP with HA-tagged UFMylation components UBA5, UFC1, UFL1, DDRGK1, and UFM1 in HEK293T cells as described previously,[30] and the results showed that exogenous YAP was covalently conjugated to both wild-type (UFM1WT) and active UFM1 (UFM1ΔC2), but not to defective UFM1 (UFM1ΔC3) (Figures 2C and S2D). Furthermore, we observed that compound 8.5 significantly inhibited the modification of YAP by UFMylation (Figure S1E). Concordantly, we further found that endogenous YAP in aortic ECs from mice can be UFMylated by UFM1 (Figure 2D). The subcellular localization of YAP as a co-transcriptional activator is important for its function.[38] Our results showed that in senescent HUVECs, YAP appeared to have a pronounced nuclear localization and the co-localization of YAP and UFM1 was predominantly in the nucleus (Figures 2E and 2F). Furthermore, the results of the *in situ* proximity ligation assay (PLA) experiments also demonstrated that UFM1-modified YAP was elevated in senescent HUVECs and predominantly distributed in the nucleus (Figure 2G). Taken together, these results indicate that UFMylation and YAP activities are increased during EC senescence and suggest that UFMylation of YAP may be a mechanism of EC senescence.

UFMylation of YAP promotes its stability and inhibition of UFMylation could prevent endothelial cell senescence

UFMylation, a ubiquitin-like modification, has been reported to be a modulator of protein stability.[23] To further explore the role of UFMylation of YAP, we employed siRNA against (UFM1 specific ligase 1) UFL1 or UFM1 in HUVECs, silencing UFL1 and UFM1, respectively. The results suggest that deficiency of either UFL1 or UFM1 leads to reduced levels of YAP (Figures 3A and 3B), and implied that UFMylation of YAP could stably increase its stability. We treated young and senescent HUVECs with cycloheximide (CHX) at indicated times and observed that the rate of YAP degradation was significantly reduced in senescent cells compared to younger cells (Figures 3C and 3D). Moreover, compound 8.5, an inhibitor of E1 of UFMylation (UBA5),[39] could dramatically increase the rate of YAP degradation in senescent HUVECs (Figures 3E and 3F). Together, these results suggest that the rate of YAP degradation is significantly reduced in senescent HUVECs and that inhibition of the activity of the UFMylation could increase the rate of YAP degradation. Thus, the YAP-UFMylation axis may be an anti-ECs senescence target. In order to clarify the role of UFMylation in ECs senescence, compound 8.5 and VP were applied to H_2O_2-induced senescent HUVECs. We found that both VP and compound 8.5 inhibited H_2O_2-induced EC senescence specifically as evidenced by a decrease in P16, P21, P53, and VCAM-1, as well as a decrease in SA-β-Gal-positive cells (Figures 3G–3J). In addition, the two compounds were used in conjunction with each other with a certain superimposed effect (Figure 3J).

Inhibition of UFMylation could retard cardiovascular aging in aged mice

There is a strong link between EC function and cardiovascular aging. So, to further validate the role of compound 8.5 in the aging of the cardiovascular system in aged mice, we administered compound 8.5 (0.25 mg/kg/d) intraperitoneally for 3 weeks in aged mice. Vascular stiffness and cardiac function are important indicators of aging in the cardiovascular system, we found that compound 8.5 significantly improved cardiac function in aged mice as evidenced by an increase in ejection fraction (EF), fractional shortening (FS), and improvement in cardiac fibrosis (Figures S2A–S2D). However, there was no significant change in the weight of the mice (Figure S2E). In addition, the vascular stiffness of the aortic arch, carotid artery and abdominal aorta also demonstrated a significant improvement in compound 8.5 treatment aged mice, as shown by decrease in pulse wave velocity (PWV) and increase in vascular strain (Figure 4A). Vascular collagen deposition is also a major feature of vascular aging, and the application of compound 8.5 also significantly reduced vascular collagen deposition in aged mice (Figures 4B and 4C). More importantly, in aortic ECs from aged mice treated with compound 8.5, the senescence-related markers P16, P21, P53, and VCAM-1 were also significantly reduced, in line with the reduction in YAP protein levels (Figures 4D and 4E). These suggest that YAP-UFMylation is a potential target for anti-vascular aging. Although VP has strong anti-aging effects, it has been reported to have strong cytotoxicity that induces apoptosis,[40] so the potential for clinical application is low, compound 8.5 may be a better choice for anti-vascular aging.

Compound 8.5 reduces the expression of SASP genes in the aortas of aged mice

To investigate the downstream target genes of compound 8.5 in the arteries of mice, we have used RNA sequencing (RNA-seq) technology to compare the transcriptomic profiles of the aortas of aged mice and aged mice treated with compound 8.5. We identified 807 genes upregulated and 1252 genes downregulated (fold change >2 and adjusted p value <0.05) in the aorta

(C and D) The proliferation of HUVECs PDL at 10 and 30 were treated with cycloheximide (CHX) (10 μM) for the indicated time. Immunoblotting and quantifying the protein level of YAP, $n = 3$, p values correspond to two-way ANOVA with Sidak's multiple comparisons test.
(E and F) Proliferation of HUVECs PDL at 30 were treated with vehicle or compound 8.5 (20 μM) for 12 h, followed by treated with CHX (10 μM) for the indicated time. Immunoblotting and quantifying the protein level of YAP, $n = 3$, p values correspond to two-way ANOVA with Sidak's multiple comparisons test.
(G and J) Proliferation of HUVECs PDL at 10 were treated with vehicle or H_2O_2 (100 μM) for 12 h, followed by treated with vehicle, verteporfin (0.5 μM), compound 8.5 (20 μM) or verteporfin (0.5 μM), and compound 8.5 (20 μM) for 12 h. $n = 3$.
(G and H) Immunoblotting and quantifying the indicated protein levels.
(I and J) SA-β-Gal staining and quantitative analysis of senescent cells, scale bars: 40 μm, $n = 6$, p values correspond to one-way ANOVA with Tukey's multiple comparisons test.
All data are represented as mean ± SEM. *, $p \leq 0.05$; **, $p \leq 0.01$; ***, $p \leq 0.001$.

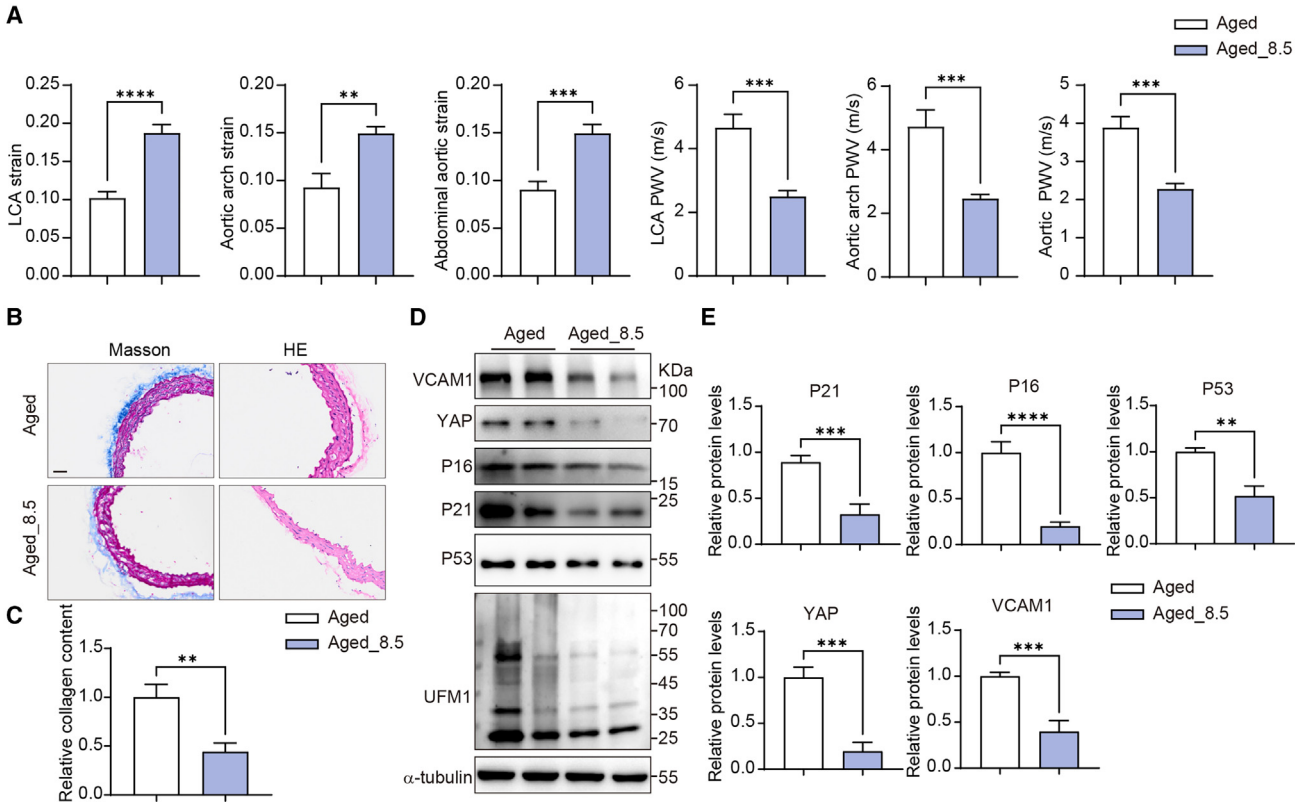

Figure 4. Inhibition of UFMylation have a role in the prevention of cardiovascular system aging

(A–E) 24 (aged) months mice were administered PBS or compound 8.5 (0.25 mg/kg/d) intraperitoneally for 3 weeks. *p* values correspond to unpaired two-tailed Student's t test.

(A) Quantitative analysis of strain and pulse wave velocity (PWV) in the left carotid artery (LCA), aortic arch, and abdominal aorta of mice, $n = 8$.

(B) Masson and HE staining of aortic cross section.

(C) Quantitative analysis of Masson staining, $n = 6$.

(D and E) Immunoblotting and quantification of the indicated protein from mouse aortic endothelial cells, $n = 6$.

All data are represented as mean ± SEM. **, $p \leq 0.01$; ***, $p \leq 0.001$; ****, $p \leq 0.0001$.

of the compound 8.5-treated mice compared to control mice (Figures 5A and 5B). A KEGG (Kyoto Encyclopedia of Genes and Genomes) enrichment analysis of the downregulated genes was performed by which we found that the downregulated genes were mainly focused on cytokine-cytokine receptor interaction, cell adhesion molecules and chemokine signaling pathway (Figure 5C). Meanwhile, YAP as a co-transcriptional activator has been reported to regulate the expression of several cytokines and adhesion factors such as IL-6, ICAM-1, and VCAM-1, which are closely associated with vascular aging.[16,41–44] On further analysis of the differential genes, we found that senescence-associated secretory phenotype (SASP)-associated gene, cell cycle-associated gene and YAP target gene were significantly downregulated in the aortas of compound 8.5-treated mice (Figure 5D). We validated the RNA-seq-sequenced SASP-related genes by reverse transcription polymerase chain reaction (RT-qPCR). As shown in Figure 5E, compound 8.5 significantly downregulated the expression of *Mmp19*, *Il6*, *Il15*, *Il7*, *Il18*, *Cxcl1*, and *Ccl17* in vascular ECs in aged mice, whereas as seen in Figure S3A, compound 8.5 significantly downregulated the expression of *MMP19*, *IL6*, *IL15*, *IL7*, *IL18*, *CXCL1*, and *CCL2* in senescent HUVECs. Therefore, our results suggest that YAP may directly regulate the expression of SASP genes to induced vascular senescence, whereas compound 8.5 reversed it by inhibiting UFMylation of YAP.

DISCUSSION

The Hippo signaling pathway has been shown to play an important role in organ size control and tumorigenesis, while YAP, a key downstream effector, has been proved essential for development and multiple CVDs, particularly atherosclerosis, a major aging-related CVD.[17,45,46] Treatment with VP, an inhibitor of YAP, has been shown to attenuate fibroblast senescence and reduce the number of senescent cells in the organs of aged mice.[21] The main mechanism of ECs YAP in promoting atherosclerosis is that YAP translocation into the nucleus promotes ECs activation with an inflammatory phenotype.[17] Meanwhile, with age, oxidative stress and the consequent activation of inflammatory signaling pathways sensitive to redox responses are thought to be associated with the inflammatory process in aging vascular. Following this, activation of vascular ECs results

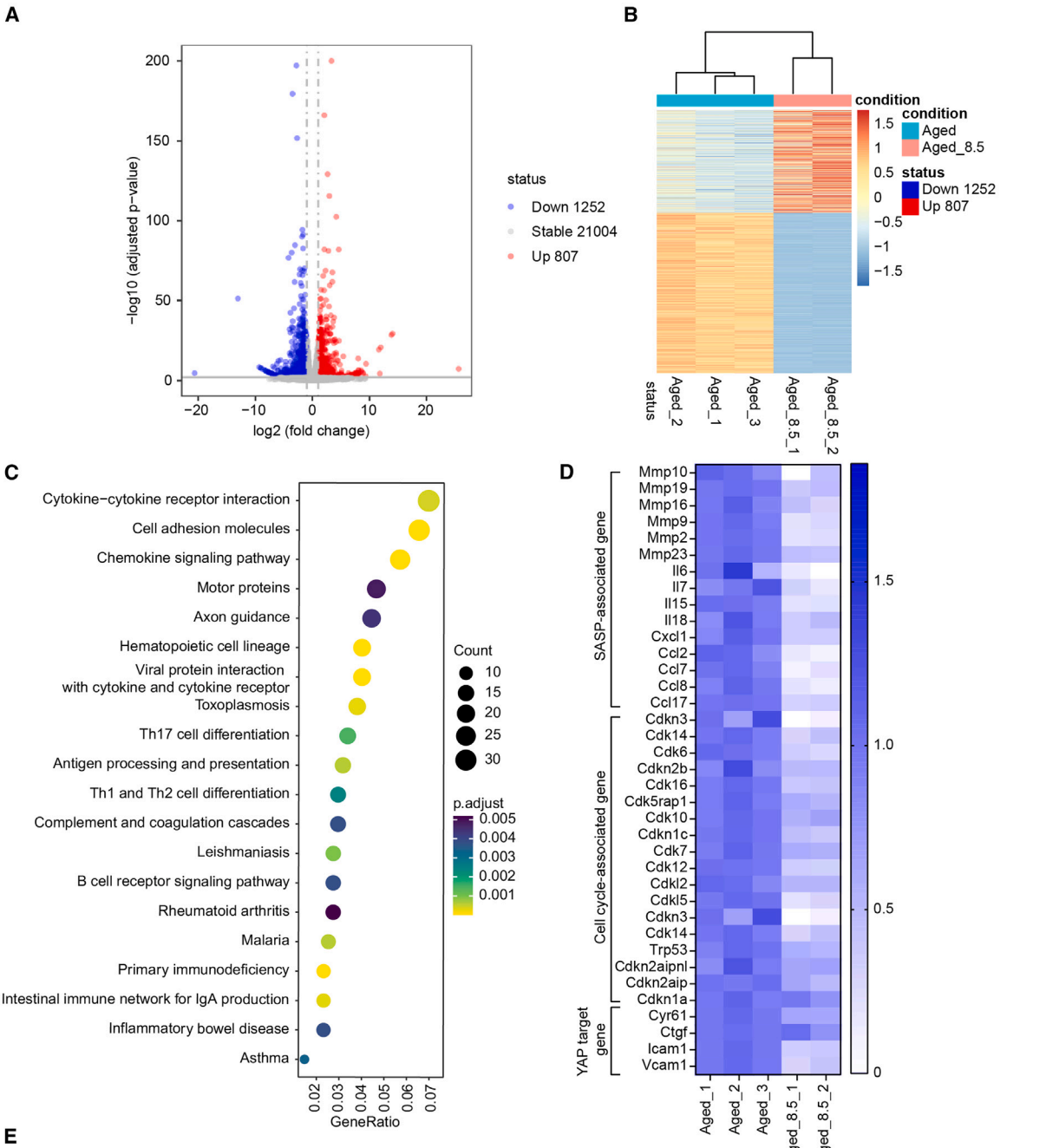

(legend on next page)

in a pro-inflammatory phenotype, secreting large amounts of inflammatory factors and the SASP.[47] These studies suggest that dysfunction due to inflammatory activation of ECs is a common characteristic of vascular aging and atherosclerosis. Recent research shows that nucleoporin93 (Nup93) limits YAP activity to prevent chronic inflammation-induced EC senescence.[22] Now, our findings revealed that YAP and UFM1-modified YAP were elevated in senescent ECs, displaying a pronounced nuclear localization with only a minimal proportion present in the cytoplasm, that UFMylation of YAP promotes natural and oxidative stress-induced EC senescence, and that inhibiting UFMylation of YAP delays it and ameliorates the cardiovascular aging phenotype in aged mice.

PTMs, such as phosphorylation, ubiquitination, sumoylation, acetylation, glycosylation, and others, could regulate protein stability, activation, inactivation, or subcellular localization. Meanwhile, growing evidence suggests that YAP is tightly regulated by various types of PTMs.[37] For example, phosphorylation of the serine 127 and 397 sites of YAP causes its retention in the cytoplasm and its degradation, whereas phosphorylation of tyrosine 357 promotes its translocation to the nucleus and modulates the expression of downstream target gene[31,48,49]; SCFSKP2 E3 ligase complex (SKP2)-mediated K63 polyubiquitination of YAP enhances its interaction with its nuclear binding partner TEAD[50]; O-GlcNAcylation at the YAP threonine 241 site increases its protein stability.[51] UFMylation, a ubiquitin-like modification, that affects protein-protein interactions, protein stability, and thus the function of protein targets, and plays an important role in a variety of cellular biological processes, as yet only a few substrates have been identified.[52] Interestingly, here, we identified a PTM of YAP, UFMylation, could increase protein stability of YAP and UFM1-modified YAP was elevated in senescent ECs and predominantly distributed in the nucleus. The upregulation of UFM1 expression in senescent EC facilitates UFMylation of YAP, which in turn promotes its nuclear translocation. However, in this study we did not identify the specific amino acid sites at which UFMylation of YAP occurs, and that will be the focus of our future work.

Our results suggest that targeting YAP as well as YAP-UFMylation are efficient approaches to attenuate EC senescence. The currently identified YAP inhibitor, VP which is clinically used in photodynamic therapy for the treatment of neovascular macular degeneration, is primarily a regional drug with high cytotoxicity not adapted for systemic administration,[53–55] and thus has little clinical value for use in anti-vascular aging. Compound 8.5 selectively inhibits UBA5, E1 of UFMylation, inhibits YAP-UFMylation and promotes ECs YAP degradation, thus suppressed ECs senescence, which has potential application in anti-vascular aging. There have been very few studies on compound 8.5 in the cardiovascular system. Whereas YAP has an important role in a variety of CVDs, it would be of potential value to further explore whether compound 8.5 has a specific protective role in other YAP-associated CVDs such as atherosclerosis.

In conclusion, we found that YAP was significantly upregulated in senescent ECs and promoted its senescence. On the mechanism, we identified YAP as a substrate for UFMylation and found that UFMylation of YAP increased its protein stability, and targeting YAP-UFMylation suppresses EC senescence and improves cardiovascular aging phenotype in aged mice, which may be an effective approach for anti-vascular aging.

Limitations of the study

Using *in vivo* and *in vitro* experiments, we found that compound 8.5 was able to block YAP-UFMylation and promote YAP degradation in ECs, thereby preventing EC senescence. Sex differences in vascular aging have been shown in previous studies.[56] However, our study was carried out in male mice only, and it remains to be tested whether the mechanism we have observed is also applicable to female mice; this is a limitation of our work. We have not identified the specific amino acid sites at which UFMylation of YAP occurs, which is another limitation of the study.

RESOURCE AVAILABILITY

Lead contact

Further information and requests for resources and reagents should be directed to and will be fulfilled by the lead contact, Prof. Hu Wang (wanghu19860315@163.com).

Materials availability

This study did not generate new unique reagents.

Data and code availability

- RNA-seq data have been deposited to the Gene Expression Omnibus (GEO) database (https://www.ncbi.nlm.nih.gov/geo/) under the accession number GSE273828 and are publicly available. Original western blot images have been deposited at Mendeley (https://data.mendeley.com/preview/2c97jkvx9c?a=f6996a71-5f0f-469d-84af-f85dbb1ea464) and are publicly available as of the date of publication.
- This paper does not report original code.
- Any additional information required to reanalyze the data reported in this paper is available from the lead contact upon request.

ACKNOWLEDGMENTS

This work was supported by the National Key R&D Program of China (2021YFA1102800) and by National Natural Science Foundation of China (92249304, 82030039, 82230047, 82300474, 82372916, and 82301746).

Figure 5. Inhibition of UFMylation repressed the expression of genes associated with SASP in the aortas of aged mice

(A–E) Twenty-four (aged) months mice were administered PBS or compound 8.5 (0.25 mg/kg/d) intraperitoneally for 3 weeks, followed by the aorta of the mice were used to perform RNA sequencing (RNA-seq).

(A) The distribution of the DEGs is shown as a volcano plot. Fold change >2 and adjusted p value <0.05 were used as up- or downregulated. Different colors indicate the relative fold expression of each gene: red dots represent up-regulated genes, green dots represent downregulated genes, and gray dots indicate no change in expression levels.

(B) Heatmap showing DEGs fold change >2 and adjusted p value < 0.05.

(C) Top 20 pathways of downregulated genes from KEGG pathway analysis.

(D) A heatmap showing the relative expression levels of the SASP-associated gene, the cell cycle-associated gene and the YAP target gene in two groups of mice.

(E) RT-qPCR analysis of the indicated gene expression in mouse vascular endothelial cells, $n = 4$, p values correspond to unpaired two-tailed Student's t test. All data are represented as mean ± SEM. ns, $p > 0.05$; *, $p \leq 0.05$; **, $p \leq 0.01$.

AUTHOR CONTRIBUTIONS

Conceptualization, Y.L., Y.B., J.Z., and H.W.; methodology, Y.L., M.Z., and S.W.; data collection and analysis, Y.L., M.Z., A.W., Z.W., and S.W.; funding acquisition, J.Z., H.W., Y.L., and A.W.; supervision, J.Z. and H.W.; writing, Y.L., J.Z., and H.W.; review and approval, all authors read and approved the final manuscript.

DECLARATION OF INTERESTS

The authors declare no competing interests.

STAR★METHODS

Detailed methods are provided in the online version of this paper and include the following:

- KEY RESOURCES TABLE
- EXPERIMENTAL MODEL AND STUDY PARTICIPANT DETAILS
  - Cell lines
  - Animals
- METHOD DETAILS
  - Extraction proteins and western blot analysis
  - Extract protein from arterial endothelial cells
  - UFMylation detection
  - Immunostaining
  - *In situ* proximity ligation assay
  - Cell culture and transfection
  - Senescence-associated β-Galactosidase (SA-β-Gal) staining
  - Animals and treatment
  - RNA-seq
- QUANTIFICATION AND STATISTICAL ANALYSIS

SUPPLEMENTAL INFORMATION

Supplemental information can be found online at https://doi.org/10.1016/j.isci.2025.111854.

Received: July 24, 2024
Revised: October 30, 2024
Accepted: January 17, 2025
Published: January 21, 2025

REFERENCES

1. Roth, G.A., Mensah, G.A., Johnson, C.O., Addolorato, G., Ammirati, E., Baddour, L.M., Barengo, N.C., Beaton, A.Z., Benjamin, E.J., Benziger, C.P., et al. (2020). Global Burden of Cardiovascular Diseases and Risk Factors, 1990-2019: Update From the GBD 2019 Study. J. Am. Coll. Cardiol. *76*, 2982–3021. https://doi.org/10.1016/j.jacc.2020.11.010.
2. Mazurek, R., Dave, J.M., Chandran, R.R., Misra, A., Sheikh, A.Q., and Greif, D.M. (2017). Vascular Cells in Blood Vessel Wall Development and Disease. Adv. Pharmacol. *78*, 323–350. https://doi.org/10.1016/bs.apha.2016.08.001.
3. Peng, Z., Shu, B., Zhang, Y., and Wang, M. (2019). Endothelial Response to Pathophysiological Stress. Arterioscler. Thromb. Vasc. Biol. *39*, e233–e243. https://doi.org/10.1161/ATVBAHA.119.312580.
4. Han, Y., and Kim, S.Y. (2023). Endothelial senescence in vascular diseases: current understanding and future opportunities in senotherapeutics. Exp. Mol. Med. *55*, 1–12. https://doi.org/10.1038/s12276-022-00906-w.
5. Erusalimsky, J.D., and Kurz, D.J. (2006). Endothelial cell senescence. Handb. Exp. Pharmacol. *1*, 213–248. https://doi.org/10.1007/3-540-36028-x_7.
6. Dominic, A., Banerjee, P., Hamilton, D.J., Le, N.T., and Abe, J.I. (2020). Time-dependent replicative senescence vs. disturbed flow-induced premature aging in atherosclerosis. Redox Biol. *37*, 101614. https://doi.org/10.1016/j.redox.2020.101614.
7. North, B.J., and Sinclair, D.A. (2012). The intersection between aging and cardiovascular disease. Circ. Res. *110*, 1097–1108. https://doi.org/10.1161/CIRCRESAHA.111.246876.
8. Camici, G.G., Savarese, G., Akhmedov, A., and Lüscher, T.F. (2015). Molecular mechanism of endothelial and vascular aging: implications for cardiovascular disease. Eur. Heart J. *36*, 3392–3403. https://doi.org/10.1093/eurheartj/ehv587.
9. Bloom, S.I., Islam, M.T., Lesniewski, L.A., and Donato, A.J. (2023). Mechanisms and consequences of endothelial cell senescence. Nat. Rev. Cardiol. *20*, 38–51. https://doi.org/10.1038/s41569-022-00739-0.
10. Belcastro, E., Rehman, A.U., Remila, L., Park, S.H., Gong, D.S., Anton, N., Auger, C., Lefebvre, O., Goetz, J.G., Collot, M., et al. (2021). Fluorescent nanocarriers targeting VCAM-1 for early detection of senescent endothelial cells. Nanomedicine. *34*, 102379. https://doi.org/10.1016/j.nano.2021.102379.
11. Zhao, B., Tumaneng, K., and Guan, K.L. (2011). The Hippo pathway in organ size control, tissue regeneration and stem cell self-renewal. Nat. Cell Biol. *13*, 877–883. https://doi.org/10.1038/ncb2303.
12. Meng, Z., Moroishi, T., and Guan, K.L. (2016). Mechanisms of Hippo pathway regulation. Genes Dev. *30*, 1–17. https://doi.org/10.1101/gad.274027.115.
13. Zhou, Q., Li, L., Zhao, B., and Guan, K.L. (2015). The hippo pathway in heart development, regeneration, and diseases. Circ. Res. *116*, 1431–1447. https://doi.org/10.1161/CIRCRESAHA.116.303311.
14. Wang, Y., Hu, G., Liu, F., Wang, X., Wu, M., Schwarz, J.J., and Zhou, J. (2014). Deletion of yes-associated protein (YAP) specifically in cardiac and vascular smooth muscle cells reveals a crucial role for YAP in mouse cardiovascular development. Circ. Res. *114*, 957–965. https://doi.org/10.1161/CIRCRESAHA.114.303411.
15. Zhang, H., von Gise, A., Liu, Q., Hu, T., Tian, X., He, L., Pu, W., Huang, X., He, L., Cai, C.L., et al. (2014). Yap1 is required for endothelial to mesenchymal transition of the atrioventricular cushion. J. Biol. Chem. *289*, 18681–18692. https://doi.org/10.1074/jbc.M114.554584.
16. Wang, K.C., Yeh, Y.T., Nguyen, P., Limqueco, E., Lopez, J., Thorossian, S., Guan, K.L., Li, Y.S.J., and Chien, S. (2016). Flow-dependent YAP/TAZ activities regulate endothelial phenotypes and atherosclerosis. Proc. Natl. Acad. Sci. USA *113*, 11525–11530. https://doi.org/10.1073/pnas.1613121113.
17. Wang, L., Luo, J.Y., Li, B., Tian, X.Y., Chen, L.J., Huang, Y., Liu, J., Deng, D., Lau, C.W., Wan, S., et al. (2016). Integrin-YAP/TAZ-JNK cascade mediates atheroprotective effect of unidirectional shear flow. Nature *540*, 579–582. https://doi.org/10.1038/nature20602.
18. Yao, L., He, J., Li, B., Yan, M., Wang, H., Tan, L., Liu, M., Lv, X., Lv, H., Zhang, X., et al. (2019). Regulation of YAP by Mammalian Target of Rapamycin Complex 1 in Endothelial Cells Controls Blood Pressure Through $COX\text{-}2$/$mPGES\text{-}1$/PGE_2 Cascade. Hypertension *74*, 936–946. https://doi.org/10.1161/HYPERTENSIONAHA.119.12834.
19. Ikeda, S., Mukai, R., Mizushima, W., Zhai, P., Oka, S.I., Nakamura, M., Del Re, D.P., Sciarretta, S., Hsu, C.P., Shimokawa, H., and Sadoshima, J. (2019). Yes-Associated Protein (YAP) Facilitates Pressure Overload-Induced Dysfunction in the Diabetic Heart. JACC. Basic Transl. Sci. *4*, 611–622. https://doi.org/10.1016/j.jacbts.2019.05.006.
20. Liu, Y., Li, M., Lv, X., Bao, K., Yu Tian, X., He, L., Shi, L., Zhu, Y., and Ai, D. (2022). Yes-Associated Protein Targets the Transforming Growth Factor beta Pathway to Mediate High-Fat/High-Sucrose Diet-induced Arterial Stiffness. Circ. Res. *130*, 851–867. https://doi.org/10.1161/CIRCRESAHA.121.320464.
21. Anerillas, C., Mazan-Mamczarz, K., Herman, A.B., Munk, R., Lam, K.W.G., Calvo-Rubio, M., Garrido, A., Tsitsipatis, D., Martindale, J.L., Altés, G., et al. (2023). The YAP-TEAD complex promotes senescent cell survival

by lowering endoplasmic reticulum stress. Nat. Aging *3*, 1237–1250. https://doi.org/10.1038/s43587-023-00480-4.

22. Nguyen, T.D., Rao, M.K., Dhyani, S.P., Banks, J.M., Winek, M.A., Michalkiewicz, J., and Lee, M.Y. (2023). Nucleoporin93 (Nup93) Limits Yap Activity to Prevent Endothelial Cell Senescence. Preprint at bioRxiv, 2023.11.10.566598. https://doi.org/10.1101/2023.11.10.566598.
23. Gerakis, Y., Quintero, M., Li, H., and Hetz, C. (2019). The UFMylation System in Proteostasis and Beyond. Trends Cell Biol. *29*, 974–986. https://doi.org/10.1016/j.tcb.2019.09.005.
24. Liang, Z., Ning, R., Wang, Z., Kong, X., Yan, Y., Cai, Y., He, Z., Liu, X.G., Zou, Y., and Zhou, J. (2024). The emerging roles of UFMylation in the modulation of immune responses. Clin. Transl. Med. *14*, e70019. https://doi.org/10.1002/ctm2.70019.
25. Zhou, X., Mahdizadeh, S.J., Le Gallo, M., Eriksson, L.A., Chevet, E., and Lafont, E. (2024). UFMylation: a ubiquitin-like modification. Trends Biochem. Sci. *49*, 52–67. https://doi.org/10.1016/j.tibs.2023.10.004.
26. Liu, J., Guan, D., Dong, M., Yang, J., Wei, H., Liang, Q., Song, L., Xu, L., Bai, J., Liu, C., et al. (2020). UFMylation maintains tumour suppressor p53 stability by antagonizing its ubiquitination. Nat. Cell Biol. *22*, 1056–1063. https://doi.org/10.1038/s41556-020-0559-z.
27. Balce, D.R., Wang, Y.T., McAllaster, M.R., Dunlap, B.F., Orvedahl, A., Hykes, B.L., Jr., Droit, L., Handley, S.A., Wilen, C.B., Doench, J.G., et al. (2021). UFMylation inhibits the proinflammatory capacity of interferon-gamma-activated macrophages. Proc. Natl. Acad. Sci. USA *118*, e2011763118. https://doi.org/10.1073/pnas.2011763118.
28. Li, J., Yue, G., Ma, W., Zhang, A., Zou, J., Cai, Y., Tang, X., Wang, J., Liu, J., Li, H., and Su, H. (2018). Ufm1-Specific Ligase Ufl1 Regulates Endoplasmic Reticulum Homeostasis and Protects Against Heart Failure. Circ. Heart Fail. *11*, e004917. https://doi.org/10.1161/CIRCHEARTFAILURE.118.004917.
29. Xu, X., Huang, W., Bryant, C.N., Dong, Z., Li, H., and Wu, G. (2024). The ufmylation cascade controls COPII recruitment, anterograde transport, and sorting of nascent GPCRs at ER. Sci. Adv. *10*, eadm9216. https://doi.org/10.1126/sciadv.adm9216.
30. Zhou, J., Ma, X., He, X., Chen, B., Yuan, J., Jin, Z., Li, L., Wang, Z., Xiao, Q., Cai, Y., et al. (2023). Dysregulation of PD-L1 by UFMylation imparts tumor immune evasion and identified as a potential therapeutic target. Proc. Natl. Acad. Sci. USA *120*, e2215732120. https://doi.org/10.1073/pnas.2215732120.
31. Li, B., He, J., Lv, H., Liu, Y., Lv, X., Zhang, C., Zhu, Y., and Ai, D. (2019). c-Abl regulates YAPY357 phosphorylation to activate endothelial atherogenic responses to disturbed flow. J. Clin. Invest. *129*, 1167–1179. https://doi.org/10.1172/JCI122440.
32. Liu, M., Yan, M., Lv, H., Wang, B., Lv, X., Zhang, H., Xiang, S., Du, J., Liu, T., Tian, Y., et al. (2020). Macrophage K63-Linked Ubiquitination of YAP Promotes Its Nuclear Localization and Exacerbates Atherosclerosis. Cell Rep. *32*, 107990. https://doi.org/10.1016/j.celrep.2020.107990.
33. Jia, M., Li, Q., Guo, J., Shi, W., Zhu, L., Huang, Y., Li, Y., Wang, L., Ma, S., Zhuang, T., et al. (2022). Deletion of BACH1 Attenuates Atherosclerosis by Reducing Endothelial Inflammation. Circ. Res. *130*, 1038–1055. https://doi.org/10.1161/CIRCRESAHA.121.319540.
34. Pang, Z.D., Sun, X., Bai, R.Y., Han, M.Z., Zhang, Y.J., Wu, W., Zhang, Y., Lai, B.C., Zhang, Y., Wang, Y., et al. (2023). YAP-galectin-3 signaling mediates endothelial dysfunction in angiotensin II-induced hypertension in mice. Cell. Mol. Life Sci. *80*, 38. https://doi.org/10.1007/s00018-022-04623-5.
35. Lin, M., Yuan, W., Su, Z., Lin, C., Huang, T., Chen, Y., and Wang, J. (2018). Yes-associated protein mediates angiotensin II-induced vascular smooth muscle cell phenotypic modulation and hypertensive vascular remodelling. Cell Prolif. *51*, e12517. https://doi.org/10.1111/cpr.12517.
36. Menghini, R., Casagrande, V., Cardellini, M., Martelli, E., Terrinoni, A., Amati, F., Vasa-Nicotera, M., Ippoliti, A., Novelli, G., Melino, G., et al. (2009). MicroRNA 217 modulates endothelial cell senescence via silent information regulator 1. Circulation *120*, 1524–1532. https://doi.org/10.1161/CIRCULATIONAHA.109.864629.
37. Yan, F., Qian, M., He, Q., Zhu, H., and Yang, B. (2020). The posttranslational modifications of Hippo-YAP pathway in cancer. Biochim. Biophys. Acta. Gen. Subj. *1864*, 129397. https://doi.org/10.1016/j.bbagen.2019.07.006.
38. Totaro, A., Panciera, T., and Piccolo, S. (2018). YAP/TAZ upstream signals and downstream responses. Nat. Cell Biol. *20*, 888–899. https://doi.org/10.1038/s41556-018-0142-z.
39. da Silva, S.R., Paiva, S.L., Bancerz, M., Geletu, M., Lewis, A.M., Chen, J., Cai, Y., Lukkarila, J.L., Li, H., and Gunning, P.T. (2016). A selective inhibitor of the UFM1-activating enzyme, UBA5. Bioorg. Med. Chem. Lett. *26*, 4542–4547. https://doi.org/10.1016/j.bmcl.2015.10.015.
40. Chen, M., Zhong, L., Yao, S.F., Zhao, Y., Liu, L., Li, L.W., Xu, T., Gan, L.G., Xiao, C.L., Shan, Z.L., and Liu, B.Z. (2017). Verteporfin Inhibits Cell Proliferation and Induces Apoptosis in Human Leukemia NB4 Cells without Light Activation. Int. J. Med. Sci. *14*, 1031–1039. https://doi.org/10.7150/ijms.19682.
41. Yang, W., Yang, S., Zhang, F., Cheng, F., Wang, X., and Rao, J. (2020). Influence of the Hippo-YAP signalling pathway on tumor associated macrophages (TAMs) and its implications on cancer immunosuppressive microenvironment. Ann. Transl. Med. *8*, 399. https://doi.org/10.21037/atm.2020.02.11.
42. Meli, V.S., Atcha, H., Veerasubramanian, P.K., Nagalla, R.R., Luu, T.U., Chen, E.Y., Guerrero-Juarez, C.F., Yamaga, K., Pandori, W., Hsieh, J.Y., et al. (2020). YAP-mediated mechanotransduction tunes the macrophage inflammatory response. Sci. Adv. *6*, eabb8471. https://doi.org/10.1126/sciadv.abb8471.
43. Propson, N.E., Roy, E.R., Litvinchuk, A., Köhl, J., and Zheng, H. (2021). Endothelial C3a receptor mediates vascular inflammation and blood-brain barrier permeability during aging. J. Clin. Invest. *131*, e140966. https://doi.org/10.1172/JCI140966.
44. Bloom, S.I., Liu, Y., Tucker, J.R., Islam, M.T., Machin, D.R., Abdeahad, H., Thomas, T.G., Bramwell, R.C., Lesniewski, L.A., and Donato, A.J. (2023). Endothelial cell telomere dysfunction induces senescence and results in vascular and metabolic impairments. Aging Cell *22*, e13875. https://doi.org/10.1111/acel.13875.
45. Yu, F.X., Zhao, B., and Guan, K.L. (2015). Hippo Pathway in Organ Size Control, Tissue Homeostasis, and Cancer. Cell *163*, 811–828. https://doi.org/10.1016/j.cell.2015.10.044.
46. Xin, M., Kim, Y., Sutherland, L.B., Murakami, M., Qi, X., McAnally, J., Porrello, E.R., Mahmoud, A.I., Tan, W., Shelton, J.M., et al. (2013). Hippo pathway effector Yap promotes cardiac regeneration. Proc. Natl. Acad. Sci. USA *110*, 13839–13844. https://doi.org/10.1073/pnas.1313192110.
47. Ungvari, Z., Tarantini, S., Donato, A.J., Galvan, V., and Csiszar, A. (2018). Mechanisms of Vascular Aging. Circ. Res. *123*, 849–867. https://doi.org/10.1161/CIRCRESAHA.118.311378.
48. Zhao, B., Wei, X., Li, W., Udan, R.S., Yang, Q., Kim, J., Xie, J., Ikenoue, T., Yu, J., Li, L., et al. (2007). Inactivation of YAP oncoprotein by the Hippo pathway is involved in cell contact inhibition and tissue growth control. Genes Dev. *21*, 2747–2761. https://doi.org/10.1101/gad.1602907.
49. Moon, S., Kim, W., Kim, S., Kim, Y., Song, Y., Bilousov, O., Kim, J., Lee, T., Cha, B., Kim, M., et al. (2017). Phosphorylation by NLK inhibits YAP-14-3-3-interactions and induces its nuclear localization. EMBO Rep. *18*, 61–71. https://doi.org/10.15252/embr.201642683.
50. Yao, F., Zhou, Z., Kim, J., Hang, Q., Xiao, Z., Ton, B.N., Chang, L., Liu, N., Zeng, L., Wang, W., et al. (2018). SKP2- and OTUD1-regulated non-proteolytic ubiquitination of YAP promotes YAP nuclear localization and activity. Nat. Commun. *9*, 2269. https://doi.org/10.1038/s41467-018-04620-y.
51. Zhang, X., Qiao, Y., Wu, Q., Chen, Y., Zou, S., Liu, X., Zhu, G., Zhao, Y., Chen, Y., Yu, Y., et al. (2017). The essential role of YAP O-GlcNAcylation in high-glucose-stimulated liver tumorigenesis. Nat. Commun. *8*, 15280. https://doi.org/10.1038/ncomms15280.

52. Wei, Y., and Xu, X. (2016). UFMylation: A Unique & Fashionable Modification for Life. Genom. Proteom. Bioinform. *14*, 140–146. https://doi.org/10.1016/j.gpb.2016.04.001.

53. Condurat, A.L., Aminzadeh-Gohari, S., Malnar, M., Schider, N., Opitz, L., Thomas, R., Menon, V., Kofler, B., and Pruszak, J. (2023). Verteporfin-induced proteotoxicity impairs cell homeostasis and survival in neuroblastoma subtypes independent of YAP/TAZ expression. Sci. Rep. *13*, 3760. https://doi.org/10.1038/s41598-023-29796-2.

54. Kuramoto, K., Yamamoto, M., Suzuki, S., Sanomachi, T., Togashi, K., Seino, S., Kitanaka, C., and Okada, M. (2020). Verteporfin inhibits oxidative phosphorylation and induces cell death specifically in glioma stem cells. FEBS J. *287*, 2023–2036. https://doi.org/10.1111/febs.15187.

55. Brodowska, K., Al-Moujahed, A., Marmalidou, A., Meyer Zu Horste, M., Cichy, J., Miller, J.W., Gragoudas, E., and Vavvas, D.G. (2014). The clinically used photosensitizer Verteporfin (VP) inhibits YAP-TEAD and human retinoblastoma cell growth in vitro without light activation. Exp. Eye Res. *124*, 67–73. https://doi.org/10.1016/j.exer.2014.04.011.

56. Ji, H., Kwan, A.C., Chen, M.T., Ouyang, D., Ebinger, J.E., Bell, S.P., Niiranen, T.J., Bello, N.A., and Cheng, S. (2022). Sex Differences in Myocardial and Vascular Aging. Circ. Res. *130*, 566–577. https://doi.org/10.1161/CIRCRESAHA.121.319902.

STAR★METHODS

KEY RESOURCES TABLE

REAGENT or RESOURCE	SOURCE	IDENTIFIER
Antibodies		
Rabbit monoclonal anti-UFM1	Abcam	Cat# ab109305; RRID:AB_10864675
Rabbit monoclonal anti-YAP	Cell Signaling Technology	Cat# 14074; RRID:AB_2650491
Mouse monoclonal anti-YAP	Santa Cruz Biotechnology	Cat# sc-101199; RRID:AB_1131430
Rabbit monoclonal anti-P53	Cell Signaling Technology	Cat# 2527; RRID:AB_10695803)
Mouse monoclonal anti-Alpha Tubulin	Proteintech	Cat# 66031-1-Ig; RRID:AB_11042766
Rabbit monoclonal anti-p16 INK4A	Cell Signaling Technology	Cat# 18769; RRID:AB_2935679
Rabbit monoclonal anti-DYKDDDDK Tag	Cell Signaling Technology	Cat# 14793; RRID:AB_2572291
Rabbit isotype control	Cell Signaling Technology	Cat# 2729; RRID:AB_1031062
Rabbit polyclonal anti-p21	Proteintech	Cat# 10355-1-AP; RRID:AB_2077682
Rabbit polyclonal anti-UBA5	ABclonal	Cat# A15514; RRID:AB_2762915
Rabbit monoclonal anti-VCAM1	Huabio	Cat# ET1601-18; RRID:AB_3069600
Rabbit polyclonal anti-UFL1	Oasis Biofarm	Cat# OB-PRB036; RRID:AB_2938995
Anti-rabbit IgG, HRP-linked Antibody	Cell Signaling Technology	Cat# 7074; RRID:AB_2099233
Anti-mouse IgG, HRP-linked Antibody	Cell Signaling Technology	Cat# 7076; RRID:AB_330924
Bacterial and virus strains		
MCS-3xFLAG-EGFP-YAP adenovirus	GENECHEM	N/A
Chemicals, peptides, and recombinant proteins		
Cycloheximide	MedChemExpress	Cat#HY-12320
Verteporfin	MedChemExpress	Cat#HY-B0146
Compound 8.5	MedChemExpress	Cat#HY-148266
ECM culture medium	Zhong Qiao Xin Zhou Biotechnology	Cat#ZQ-1304
Trypsin-EDTA	Thermo Fisher Scientific	Cat#25200056
Protease inhibitor cocktail tablets	Roche	Cat#04693132001
Phosphatase inhibitor cocktail tablets	Roche	Cat#04906845001
PMSF	Solarbio Life Sciences	Cat#IP0280
Critical commercial assays		
TransZol Up Plus RNA Kit	TransGenBiotech	Cat# ER501-01
Lipofectamine RNAiMAX Transfection Reagent	Invitrogen	Cat# 13778030
Pierce BCA Protein Assay Kit	Thermo Fisher Scientific	Cat# 23225
ECL Western Blotting Detection Kit	Affinity	Cat# KF003
Senescence β-Galactosidase Staining Kit	Beyotime Biotechnology	Cat# C0602
Lipofectamine 3000 Transfection Reagent	Thermo Fisher Scientific	Cat# L3000001
Deposited data		
RNA-seq	This paper	GEO: GSE273828
Source data	This paper	https://data.mendeley.com/preview/2c97jkvx9c?a=f6996a71-5f0f-469d-84af-f85dbb1ea464
Experimental models: Cell lines		
HEK293T	ATCC	CRL-1573; RRID: CVCL0045
HUVEC (pooled donor) endothelial cells	Lonza	Cat# CC-2519
Experimental models: Organisms/strains		
Mouse C57BL6J	Jackson Laboratories	N/A

(*Continued on next page*)

Continued

REAGENT or RESOURCE	SOURCE	IDENTIFIER
Oligonucleotides		
Primer sequences	Table S1	N/A
YAP1 siRNA	Santa Cruz Biotechnology	Cat# sc-38637
UFM1 siRNA	Santa Cruz Biotechnology	Cat# sc-76804
UFL1 siRNA	Santa Cruz Biotechnology	Cat# sc-95134
Negative control siRNA	Santa Cruz Biotechnology	Cat# sc-37007
Recombinant DNA		
p-CMV-3xFLAG-YAP	generalbiol	N/A
pCDNA-HA-vector	This paper	N/A
pCDNA-HA-UFM1 (WT)	This paper	N/A
pCDNA-HA-UFM1 (ΔC2)	This paper	N/A
pCDNA-HA-UFM1 (ΔC3)	This paper	N/A
pCDNA-HA-UFL1	This paper	N/A
pCDNA-HA-UBA5	This paper	N/A
pCDNA-HA-UFC1	This paper	N/A
pCDNA-HA-DDRGK1	This paper	N/A
Software and algorithms		
GraphPad Prism 9	GraphPad	https://www.graphpad.com/updates/prism-900-release-notes
ImageJ	National Institutes of Health	https://imagej.en.softonic.com/
Image-Pro 7.0	National Institutes of Health	https://imagej.nih.gov/ij
Other		
Protein G and A Dynabeads	Thermo Fisher Scientific	Cat# 78609
nitrocellulose membrane	Cytiva	Cat# 10600001

EXPERIMENTAL MODEL AND STUDY PARTICIPANT DETAILS

Cell lines

Human umbilical vein endothelial cells (HUVECs) were obtained from Lonza (from pooled donors, sex: female and male), Germany cultured in Endothelial Cell Complete Medium produced by Zhong Qiao Xin Zhou Biotechnology.

The HEK293T (sex: female) was cultured in the DMEM with 10% FBS added.

Animals

Male C57BL/6J mice were obtained from Beijing Vital River Laboratory Animal Technology (Beijing, China). Mice were placed on a 12:12 h light/dark cycle under SPF facility conditions (7:00 am lights on, 7:00 pm lights off) prior to experiments. All animal experiments were conducted in strict accordance with the National Institutes of Health Guide for the Care and Use of Laboratory Animals and was approved by the Animal Care and Use Committee (HSD20221202) of Hangzhou Normal University. Cardiovascular aging has sex differences,[56] whereas our study was conducted in male mice only and it remains to be tested whether the observed mechanism also applies to female mice; this is a limitation of our work.

METHOD DETAILS

Extraction proteins and western blot analysis

Tissue or cell lysates were produced with RIPA buffer containing phosphatase inhibitor, PMSF and complete protease inhibitor cocktail. For western blot analysis, 12% Bis-Tris SDS-Gels (Bio-Rad, Hercules, CA) were used to separate the protein samples before transfer to a nitrocellulose membrane. The membrane was then blocked in 5% milk and allowed to incubate overnight at 4°C with the following primary antibodies: YAP, P16 INK4A, P21, P53, DYKDDDDK Tag, Alpha tubulin, VCAM1, UFM1, UFL1 and UBA5. Next, horseradish peroxidase-conjugated secondary antibodies were then added to the membranes (Anti-rabbit IgG, HRP-linked Antibody; Anti-mouse IgG, HRP-linked Antibody) and later visualized with the ECL Western Blotting Detection Kit using a ChemiScope3600 Mini chemiluminescence imaging system (Clinx Science Instruments; Shanghai, China).

Extract protein from arterial endothelial cells

The mice were anaesthetized with avertin (Sigma-Aldrich, ON, Canada; 0.36 mg/g body weight) and the left ventricle was perfused with saline. Subsequently, the connective and adipose tissue were removed from the aorta. The vessels were longitudinally dissected in order to expose the endothelial cells, which were then scraped gently using an ice-cold protein lysate.

UFMylation detection

To detect endogenous YAP UFMylation in mouse aortic endothelial cells, mouse aortas were isolated after euthanasia and perfusion of the left ventricle with saline, and mouse aortic endothelial cells were scraped under a microscope using lysis buffer [150 mM Tris-HCl (pH 8), 5% SDS, and 30% glycerol] and lysed in boiling lysis buffer. Lysates were diluted 20-fold in buffer A (50 mM Tris-HCl pH 8.0, 150 mM NaCl, 10 mM imidazole, 1% NP-40, 2 mM NEM and complete protease inhibitor cocktail). The supernatants were incubated with anti-YAP antibody or normal rabbit IgG overnight, followed by incubation with Protein G and A Dynabeads at 4°C for 2 hours. Immunoprecipitates were analyzed by western blotting with anti-UFM1 antibody after multiple washes with NP-40 buffer. For exogenous YAP UFMylation, we used Lipofectamine 3000 Transfection Reagent to transiently transfect the plasmids expressing the UFMylation components (UBA5, UFC1, UFL1, DDRGK1 and UFM1) and Flag-tagged YAP in HEK293T cells, and then performed immunoprecipitation with anti-Flag beads and the detection of UFMylated YAP by the UFM1 antibody.

Immunostaining

The cultured cells were washed with PBS, fixed in 4% (w/v) paraformaldehyde, permeabilized with 0.1% (v/v) Triton X-100 in PBS, blocked with 1% BSA, and incubated with the primary antibodies for 12 hours at 4°C, followed by incubation with Alexa Fluor-conjugated secondary antibodies for 1 hour at 25°C. Subsequently, the samples were mounted in Fluoroshield DAPI mounting medium. Imaging and analysis were conducted using the Zeiss confocal laser scanning microscope (LSM) 900.

In situ proximity ligation assay

A protein interaction analysis was conducted using the Duolink *In Situ* Starter Kit (Cat. No. DUO92101; Sigma-Aldrich; St. Louis, MO, USA) in accordance with the manufacturer's instructions. In brief, the cells are incubated with the primary antibodies for 12 hours at 4°C, following the fixation and permeabilization steps. Duolink PLA probes (anti-mouse and anti-rabbit) were applied to the samples for one hour at 37°C. The Duolink PLA probes (anti-mouse and anti-rabbit) were applied to the samples for one hour at 37°C. The ligation step (30 minutes, 37°C) permitted the antibody-conjugated oligonucleotides to form a DNA circle, which was then incubated with amplification buffer at 37°C for 100 minutes. Following washing, the slides were mounted on coverslips using Duolink PLA mounting medium with DAPI. Images were captured using a Zeiss confocal laser scanning microscope (LSM) 900.

Cell culture and transfection

Transfection of plasmids was conducted using Lipofectamine 3000 Transfection Reagent, while transfection of siRNA was performed using Lipofectamine RNAi MAX Transfection Reagent. Both procedures were carried out in accordance with the instructions provided by the manufacturers. The siRNA against YAP1, UFM1, UFL1 and negative control were obtained from Santa Cruz Biotechnology.

Senescence-associated β-Galactosidase (SA-β-Gal) staining

The Senescence β-Galactosidase Staining Kit (Cat. No. C0602) from Beyotime Biotechnology was used to detect cellular senescence and was performed according to the instructions. Briefly, cells were fixed in β-galactosidase fixative for 15 minutes at room temperature, then washed with PBS and incubated with staining buffer overnight at 37°C. Finally, the staining buffer was removed by adding PBS and images were captured using a Leica microscope. Image-Pro Plus (Media Cybernetics, USA) was used to quantify positive cells.

Animals and treatment

All animal care and experimentation procedures were conducted in accordance with Accreditation of Laboratory Animal Care International guidelines. The animal experiment protocol was approved by the Animal Ethics Committee of Hangzhou Normal University. The mice were procured from Beijing Vital River Laboratory Animal Technology. The male C57BL/6J mice (24 months) were administered PBS or compound 8.5 (0.25 mg/kg/d) via intraperitoneal injection. Following a three-week period, assessments were conducted to evaluate cardiac function, pulse wave velocity (PWV), and vascular strain utilizing the Vevo F2 imaging system.

RNA-seq

Mice of a 24-month age (the aged mice) were administered phosphate-buffered saline (PBS) or compound 8.5 (0.25 mg/kg/d) intraperitoneally for a period of three weeks. Thereafter, total RNA was isolated from the aortas of the mice using TransZol Up Plus RNA Kit, in accordance with the manufacturer's instructions. Poly-T oligo-attached magnetic beads were used to purify mRNA from total RNA. For quantification Kallisto was used to quantify high quality reads.

A differential expression analysis was conducted using the R package DESeq2 (v1.34.0), with differentially expressed gene thresholds set at a corrected p-value of less than 0.05 and a multiplicity of 2-fold or more. A KEGG enrichment analysis was then performed

using the R package clusterProfiler (v4.2.2). The corrected p-value was set at less than 0.05, and the heatmap was plotted using the R package pheatmap (v1.0.12). The R packages ggplot2 (v3.4.1) and ggpubr (v0.5.0) were employed for the remaining mapping.

QUANTIFICATION AND STATISTICAL ANALYSIS

For all experiments, effect sizes were estimated on the basis of preliminary data and the selected cohort sizes for all experiments were sufficient to have a power of 0.8 at an α of 0.05. Data analysis did not exclude any samples or animals and analyses were performed in a blinded fashion. Unpaired two-tailed Student's t-test was used to identify statistically significant differences between two groups; 1-way ANOVAs with Tukey's multiple-comparison test were used in Figures 1A–1C, 3B, 3H, and 3G; 2-way analysis of variance (ANOVA) with Sidak's multiple comparison test was employed in Figures 3D and 3F. All Data are represented as mean +/- SEM. ns, $P > 0.05$; *, $P \leq 0.05$; **, $P \leq 0.01$; ***, $P \leq 0.001$; ****, $P \leq 0.0001$. The figure legends for each experiment indicate the statistical tests used and exact value of n, what n represents the number of experimental repetitions conducted. Statistical analyses were performed using GraphPad Prism 9 (GraphPad Software, La Jolla, CA, USA).